



# Extremely uniform bound exciton states in nitrogen $\delta$ -doped GaAs studied by photoluminescence spectroscopy in external magnetic fields

Harada, Yukihiro

Kubo, Terutada

Inoue, Tomoya

Kojima, Osamu

Kita, Takashi

---

## (Citation)

Journal of Applied Physics, 110(8):083522-083522

## (Issue Date)

2011-10-15

## (Resource Type)

journal article

## (Version)

Version of Record

## (URL)

<https://hdl.handle.net/20.500.14094/90001617>



# Extremely uniform bound exciton states in nitrogen $\delta$ -doped GaAs studied by photoluminescence spectroscopy in external magnetic fields

Yukihiro Harada,<sup>a)</sup> Terutada Kubo, Tomoya Inoue, Osamu Kojima, and Takashi Kita  
*Department of Electrical and Electronic Engineering, Graduate School of Engineering, Kobe University,  
 Rokkodai 1-1, Nada, Kobe 657-8501, Japan*

(Received 29 July 2011; accepted 17 September 2011; published online 24 October 2011)

We studied the spatial localization of excitons bound to nitrogen (N) pairs in N  $\delta$ -doped GaAs to make clear origin of bound exciton lines. An extremely high uniformity of the emission wavelength was achieved for the exciton bound to the N pairs because of the uniform strain field in the N  $\delta$ -doped layer fabricated in the (001) plane in the atomically controlled way. The magneto-photoluminescence spectra in the Faraday configuration showed a mixing of the bright- and dark-exciton components in the exciton fine structure and diamagnetic shift. The spatial distribution of the excitons localized at different N pairs was estimated using the diamagnetic shift coefficient and confirmed by the radiative lifetime of the bright-exciton component. According to the estimated spatial distribution of bound-exciton wave function, it was found that the exciton for the 1.444-eV line is localized stronger than that for the 1.493-eV line. The strong electron confinement for the 1.444-eV line results in the reduction of exciton-phonon interaction. © 2011 American Institute of Physics. [doi:10.1063/1.3654015]

## I. INTRODUCTION

The optical and electronic properties of dilute nitride alloys are drastically modified by the interaction between the host-material conduction-band edge and nitrogen (N)-related defect levels.<sup>1–3</sup> In particular, the electronic states created by N substitution in Ga(In)As have been attracting considerable interest both from a fundamental perspective<sup>4–8</sup> and their potential device applications such as long-wavelength laser diodes,<sup>9–13</sup> low-noise avalanche photodetectors,<sup>14</sup> and multi-band solar cells.<sup>15</sup> These important applications can be realized by using properties of the strongly localized states in the infrared region. It is noted that the electronic states sensitively depend on the N configurations and their homogeneity.<sup>16</sup> Generally, N in GaAs exhibits surprisingly various configurations with their own electronic states. Therefore, the distribution of N configurations and their energy level play a key role in determining the detailed electronic properties such as the effective mass and  $g$  factor of dilute nitride alloys.<sup>16</sup> Unfortunately, there has been no way how do we control the N configurations and their energy level of dilute nitride alloys until we reported in Ref. 17.

On the other hand, in the impurity limit, N atoms act as isoelectronic traps below the conduction-band edge in Ga(In)As (Refs. 17–21) and GaP.<sup>22–25</sup> The emission wavelength of exciton bound to the isoelectronic trap is uniquely determined by a combination of the host material and the impurity centers. The energy levels of the N-pair centers in GaP are well known,<sup>22,23</sup> whereas the origin of those in GaAs is unclear; Makimoto *et al.* assigned the bound exciton lines with N pairs based on the emission wavelength.<sup>26</sup> However, it has been shown by empirical pseudopotential calculations that the energy levels created by the N pairs exhibit

nonmonotonic dependence on the pair distance.<sup>27</sup> Therefore, the distribution of N-pair levels plays a key role in determining the emission wavelengths in the impurity limit.

Recently, we developed a site-controlled N  $\delta$ -doping technique using molecular beam epitaxy (MBE) (Ref. 17) and studied the fine structure splitting of excitons bound to the N-pair centers in GaAs.<sup>28,29</sup> The linearly polarized exciton fine structure was induced by the electron-hole exchange interaction and local-strain field of the  $C_{2v}$  symmetry.<sup>28</sup> Because the  $\delta$ -doping technique restricts the N-pair formation on the growth surface, only two bound exciton lines at 1.444 and 1.493 eV were observed in N  $\delta$ -doped GaAs.<sup>17,28</sup> This result indicates that the formed N pairs are extremely uniform, which is expected to enable us to understand the bound states in detail. Furthermore, the specific emission wavelengths are advantage for the realization of solid-state photon sources. In this paper, we report on the spatial localization and uniformity of excitons bound to N pairs in N  $\delta$ -doped GaAs. The degree of exciton localization was estimated according to the diamagnetic shift and radiative lifetime. An estimation of the degree of exciton localization is essential for understanding the exciton and biexciton states in N  $\delta$ -doped GaAs.<sup>17,29</sup>

## II. SAMPLE AND EXPERIMENT

The sample was grown by MBE using As<sub>2</sub> molecular beams on (001) semi-insulating GaAs substrate after a GaAs-buffer layer. Before the N doping, a 300-nm-thick Al<sub>0.3</sub>Ga<sub>0.7</sub>As and 50-nm-thick GaAs layers were grown. The As flux was  $3.0 \times 10^{-6}$  Torr. The N doping has been performed on the  $(2 \times 4)\alpha$  surface by using active N species created in a radio-frequency plasma source from ultrapure N<sub>2</sub> gas.<sup>17</sup> The gas-flow rate was 0.37 ccm. During the N doping, the As shutter was not closed. After a growth interruption of

<sup>a)</sup>Electronic mail: y.harada@eedept.kobe-u.ac.jp.

120 s, a 50-nm-thick GaAs, 100-nm-thick  $\text{Al}_{0.3}\text{Ga}_{0.7}\text{As}$ , and 10-nm-thick GaAs-capping layers were grown. The 100-nm-thick active layer of GaAs:N was sandwiched between  $\text{Al}_{0.3}\text{Ga}_{0.7}\text{As}$  barrier layers to achieve efficient carrier capture into the N-pair centers.<sup>29</sup> This N  $\delta$ -doping technique fabricates specific N pairs utilizing the atomic ordering on the (001) surface of GaAs.<sup>17,28,29</sup> The sheet density of the N pairs estimated by photoluminescence (PL) imaging was approximately  $0.6 \mu\text{m}^{-2}$ .

Linearly polarized magneto-micro-PL measurements were carried out using a continuous-wave laser beam ( $\lambda = 484 \text{ nm}$ ) at 4.4 K. A magnetic field was applied in the [001] direction in the Faraday configuration. The PL was dispersed in an 850-mm double monochromator and detected using a liquid- $\text{N}_2$ -cooled Si-charge coupled device array. The resolution limit of our spectroscopy system was approximately  $12 \mu\text{eV}$ . The PL decay time was measured using a time-correlated single-photon counting method at 4.4 K. The excitation source was a modulated pulse laser ( $\lambda = 484 \text{ nm}$ , pulse duration: 30 ns, and repetition rate: 4 MHz). The PL was dispersed in a 220-mm double monochromator and detected by a time-to-amplitude converter system with the use of an air-cooled GaAs photomultiplier. The spectrum and time resolution limit of our setup were approximately 0.9 meV and 1 ns, respectively.

### III. RESULTS AND DISCUSSION

Figure 1(a) shows a typical macro-PL spectrum at  $T = 3.2 \text{ K}$  and  $P_{\text{exc}} = 0.06 \text{ W/cm}^2$ . Sharp emission lines at

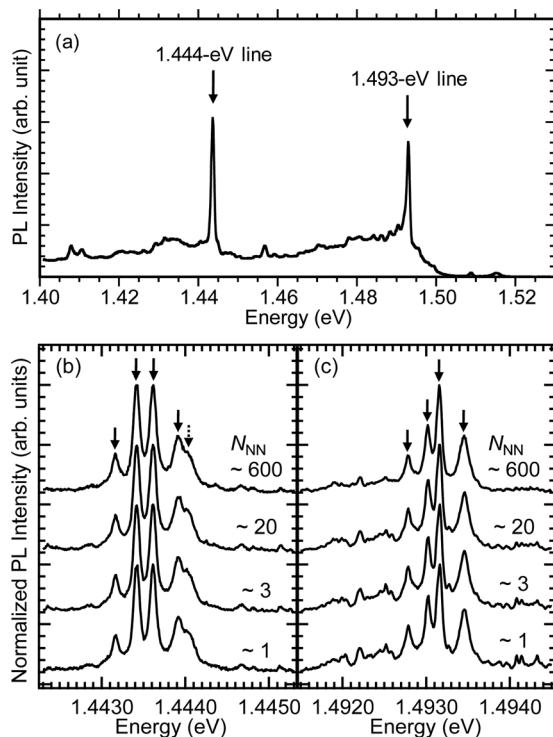


FIG. 1. (a) Typical macro-PL spectrum of N  $\delta$ -doped GaAs at  $T = 3.2 \text{ K}$  and  $P_{\text{exc}} = 0.06 \text{ W/cm}^2$ . (b) and (c) are exciton fine structure of the 1.444- and 1.493-eV lines, respectively, for different observation area at  $T = 4.4 \text{ K}$  and  $P_{\text{exc}} = 0.5 \text{ W/cm}^2$ . The N-pair numbers estimated by the PL imaging measurement were 600, 20, 3, and 1 from the top spectrum.

1.444 and 1.493 eV can be observed, as indicated by the arrows. The origin of these lines was the N pairs according to the linear polarization characteristics of the exciton fine structure.<sup>17,28,29</sup> The broad background luminescence below 1.5 eV might have resulted from the defect levels of the GaAs capping layer after N  $\delta$  doping. Figures 1(b) and 1(c) show the exciton fine structures of the 1.444- and 1.493-eV lines, respectively, for different observation areas at  $T = 4.4 \text{ K}$  and  $P_{\text{exc}} = 0.5 \text{ W/cm}^2$ . The N-pair numbers estimated by the PL imaging measurement were 600, 20, 3, and 1 from the top spectrum. The 1.493-eV line shows the four exciton fine structure, as indicated by the solid arrow, which was expected for the exciton bound to the N pair formed in the growth plane.<sup>24,28,29</sup> On the other hand, the 1.444-eV line shows an additional fine structure at the high-energy side, as indicated by the dotted arrow.<sup>29</sup> This result indicates that the N pair for the 1.444-eV line was not entirely aligned in the growth plane, which would be because of the diffusion of N atoms. In addition, these fine structures exhibited a Lorentzian-like line shape rather than a Gaussian-type structure despite the fact that we observed an ensemble of the luminescence. The homogeneous and inhomogeneous line widths were estimated to be approximately 70 and  $15 \mu\text{eV}$ , respectively, according to a pseudo-Voigt function fitting procedure<sup>30</sup> for the top spectrum of the 1.444-eV line ( $N_{\text{NN}} \sim 600$ ). This result showed the extremely high uniformity of the emission wavelength of the bound exciton in N  $\delta$ -doped GaAs. The uniformity of the emission wavelength would result from the uniform strain field in the N  $\delta$ -doped layer as compared to for conventional dilute N-doped GaAs<sup>21</sup> so that the N  $\delta$ -doping technique is considered to be suitable for suppressing the distribution of N-pair levels. The N  $\delta$ -doping technique enables the bandgap engineering.<sup>31</sup> Therefore, the controlled N levels in N  $\delta$ -doped GaAs would monotonically change the electronic properties, such as the effective mass and  $g$  factor, with increasing the amount of N for the device applications, because the random distribution of N atoms is the origin of the nonmonotonic dependence in conventional dilute N-doped GaAs.<sup>16</sup> Besides, the 1.444-eV line has nearly perfect Lorentzian line shape, whereas the 1.493-eV line has slightly asymmetric line shape as shown in Figs. 1(c) and 2(b). The asymmetric line shape of the 1.493-eV line with a larger intensity on the low-energy side would result from the different spatial localization of bound excitons between the 1.444- and 1.493-eV lines, as we discuss later. Because the effect of inhomogeneous broadening can be neglected, we focus on the luminescence from an ensemble of excitons bound to the N pairs.

Figures 2(a) and 2(b) show the magneto-PL spectra of the 1.444- and 1.493-eV lines, respectively, at  $T = 4.4 \text{ K}$  and  $P_{\text{exc}} = 0.34 \text{ W/cm}^2$ . The magnetic field was applied along [001]. The solid and dotted lines are the results for the [110] and  $[-110]$  polarizations, respectively. The bottom panels show the magnetic-field evolution of the PL-peak energies, which were extracted using a Lorentzian multipeak fitting procedure. The solid and open circles are the PL lines observed for the [110] and  $[-110]$  polarizations, respectively, at the zero magnetic field. In Fig. 2(b) for the 1.493-eV line, the exciton fine structure shows four signals observed in both

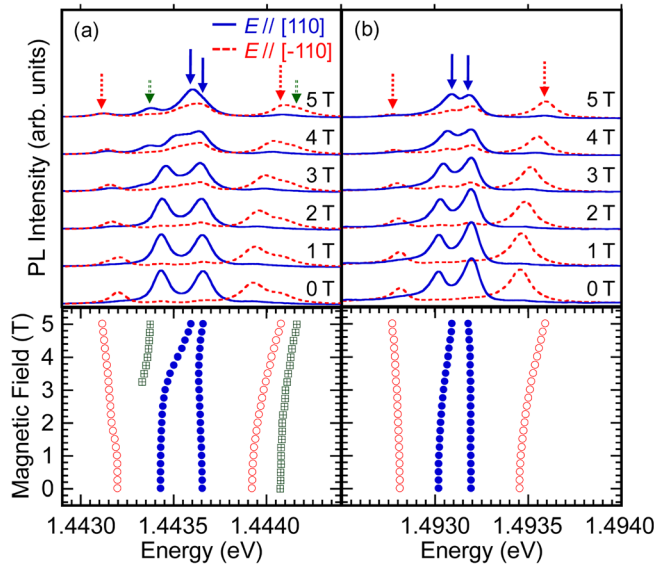


FIG. 2. (Color online) Linearly polarized magneto-PL spectra for the (a) 1.444- and (b) 1.493-eV lines, respectively, at  $T = 4.4$  K and  $P_{\text{exc}} = 0.34$  W/cm<sup>2</sup>. The magnetic field was applied along [001] in the Faraday configuration. The solid and dotted lines are the results for the [110] and [-110] polarizations, respectively. The bottom panels show the magnetic-field evolution of the PL-peak energy. The solid and open circles are the PL lines observed for the [110] and [-110] polarizations, respectively, at the zero magnetic field. The squares are unexpected PL lines in the  $C_{2v}$  symmetry in the [110] direction.

polarization directions in the high magnetic fields. This result shows the mixing between the exciton fine structures with orthogonal linear polarization components at the zero magnetic field.<sup>32</sup> On the other hand, in Fig. 2(a) for the 1.444-eV line, the exciton fine structure consists of more than four signals. The squares (short arrows) indicate unexpected PL lines in the  $C_{2v}$  symmetry in the [110] direction as shown in Fig. 1(b). The clear anticrossing behavior observed at  $\sim 1.4434$  eV at around 3 T indicates the mixing of the bright- and dark-exciton components induced by the Zeeman interaction. The mixing of these bright- and dark-exciton components also suggests that the N pair for the 1.444-eV line was not aligned in the growth plane.

The quadratic shift in energy of the exciton emission with an applied magnetic field gives information about the effects of confinement and the Coulomb interaction.<sup>33</sup> Figure 3 shows the magnetic field evolution of the average energy,  $\Delta E_{\text{ave}}$ , of the 1.444- and 1.493-eV lines.  $\Delta E_{\text{ave}}$  was defined by the average energy of the exciton fine structure indicated by the solid and open circles in Fig. 2. The diamagnetic shift coefficients for the 1.444- and 1.493-eV lines were estimated using the solid symbols to avoid the effect of the unexpected PL lines in the  $C_{2v}$  symmetry in the [110] direction. The diamagnetic shift coefficients for the 1.444- and 1.493-eV lines were estimated to be  $1.53 \pm 0.05$  and  $1.89 \pm 0.02$   $\mu\text{eV/T}^2$ , respectively. The diamagnetic shift coefficient of  $1.89$   $\mu\text{eV/T}^2$  for the 1.493-eV line is comparable to that of  $1.99$   $\mu\text{eV/T}^2$  for the 1.509-eV line observed in dilute N-doped GaAs.<sup>34</sup> These values are smaller than the values of  $8$ – $25$   $\mu\text{eV/T}^2$  for fluctuation-induced GaAs/Al<sub>0.3</sub>Ga<sub>0.7</sub>As quantum dots (QDs),<sup>35,36</sup>  $6$   $\mu\text{eV/T}^2$  for self-assembled GaAs/Al<sub>0.3</sub>Ga<sub>0.7</sub>As QDs,<sup>37</sup> and  $7$ – $11$   $\mu\text{eV/T}^2$  for self-assembled InAs/GaAs QDs<sup>38</sup> because of

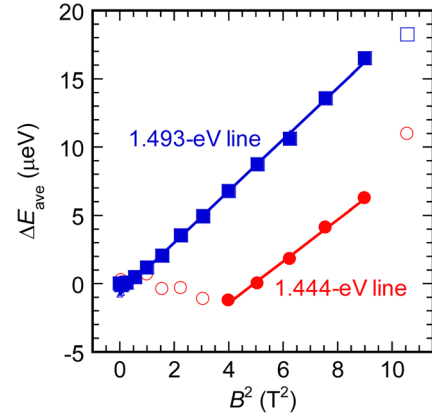


FIG. 3. (Color online) Magnetic field evolution of the average energy,  $\Delta E_{\text{ave}}$ , of the 1.444- and 1.493-eV lines.  $\Delta E_{\text{ave}}$  was defined by the average energy of the exciton fine structure indicated by the solid and open circles in Fig. 2. The circles and squares are the results for the 1.444- and 1.493-eV lines, respectively.

the strong electron confinement caused by the N isoelectronic trap. Generally, in self-assembled QDs, the splitting energy between the bright excitons is mainly determined by the long-range exchange interaction.<sup>39</sup> On the other hand, the observed small diamagnetic shift coefficients both indicate that the short-range exchange interaction and local strain field play key roles in N  $\delta$ -doped GaAs.

The diamagnetic shift coefficient  $\gamma_X$  is expressed as<sup>33</sup>

$$\gamma_X = \frac{e^2 \langle r_X^2 \rangle}{12\mu_X}, \quad (1)$$

where  $e$  is the elementary charge,  $\mu_X$  is the exciton reduced mass, and  $\langle r_X^2 \rangle$  is the exciton wave-function mean-square expectation value. According to Eq. (1), the exciton reduced mass and exciton wave-function mean-square expectation value for the 1.444-eV (1.493-eV) line are estimated to be  $0.164m_0$  ( $0.155m_0$ ) and  $4.13$  ( $4.47$ ) nm, respectively, where  $m_0$  is the electron rest mass. Here, we applied the hydrogenic 1S exciton model and used the parameters for bulk GaAs.<sup>40,41</sup> By assuming a short-range potential for the electron, the range of the electron wave function,  $\Lambda$ , is calculated by<sup>42</sup>

$$\Lambda = \sqrt{\frac{\hbar^2}{2m_e E_B}}, \quad (2)$$

where  $\hbar$  is the reduced Planck constant,  $m_e$  is the electron effective mass, and  $E_B$  is the binding energy of the bound exciton. The calculated spatial distributions of the electron for the 1.444- and 1.493-eV lines are  $0.804$  and  $1.65$  nm, respectively. This result indicates that the spatial localization of the electron for the 1.444-eV line is stronger than that for the 1.493-eV line. According to theoretical calculations indicating that only the first- and fourth-nearest neighbor N pairs create energy levels with a strong  $\Gamma$  character within the band gap,<sup>27</sup> the obtained diamagnetic shift coefficients suggest that the 1.444- and 1.493-eV lines can be attributed to the first- and fourth-nearest neighbor N pairs, respectively. The N-pair distance ratio ( $d_{\text{NN}_4}/d_{\text{NN}_1} = 2.0$ ) is comparable to the calculated ratio for the spatial distribution of the electron ( $\Lambda_{1.493 \text{ eV}}/\Lambda_{1.444 \text{ eV}} = 2.1$ ).



According to the estimated wave function of bound excitons, we discuss the asymmetric line shape of the 1.493-eV line mentioned in Figs. 1(c) and 2(b). One of the potential origin of the asymmetric line shape is the phonon sidebands due to the exciton-acoustic-phonon coupling.<sup>43,44</sup> When we assume a quasi-two-dimensional exciton wave function, the exciton-acoustic-phonon coupling becomes strong with the decrease of the lateral extension of the center-of-mass movement.<sup>43,44</sup> However, the asymmetric line shape was not observed for the localized exciton wave function of the 1.444-eV line. This result indicates the reduction of exciton-phonon interaction<sup>45</sup> due to the strong electron confinement for the 1.444-eV line. Further investigation is required to confirm the exciton-phonon interaction for bound excitons in N  $\delta$ -doped GaAs.

On the other hand, the radiative lifetime of a weakly bound exciton reflects the spatial distribution, binding energy, and effective mass of the exciton.<sup>42</sup> In order to clarify the localization of the exciton from various perspectives, we studied the radiative lifetime of these lines. Figure 4 shows the PL decay dynamics of the 1.444- and 1.493-eV lines at  $T = 4.4$  K and  $P_{\text{exc}} = 0.007$  W/cm<sup>2</sup>. The circles and squares are the results for the 1.444- and 1.493-eV lines, respectively. The dotted curve indicates the laser profile. The profiles have been normalized by the intensity at 0 ns. The PL decay profiles are found to have two decay components, which are reproduced well by double exponential fitting, as shown by the solid lines. The fast (slow) lifetimes of the 1.444- and 1.493-eV lines are 43 (43) and 11 (49) ns, respectively. The fast lifetime is considered to reflect the radiative lifetime of the bright-exciton component, whereas the slow lifetime results from the dark-exciton component and/or the background signals, as shown in Fig. 1(a). The fast lifetimes of the 1.444- and 1.493-eV lines obtained in this work were different from the values of 14.8 and 4.8 ns obtained for heavily doped GaAs:(In,N).<sup>20</sup> The faster lifetime in Ref. 20 would have resulted from the higher measurement temperature of 10 K compared to the values of 4.4 K in our measurement. The lifetime of 11 ns for the 1.493-eV line is comparable with the 10 ns for the 1.508-eV line in GaAs:N measured at 2 K.<sup>46</sup>

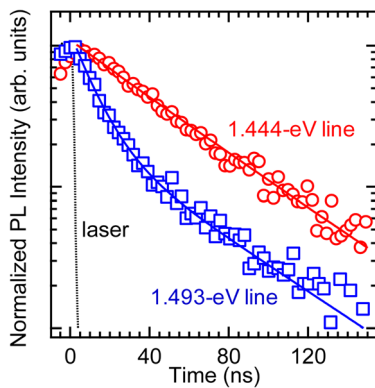


FIG. 4. (Color online) PL decay dynamics of the 1.444- and 1.493-eV lines at  $T = 4.4$  K and  $P_{\text{exc}} = 0.007$  W/cm<sup>2</sup>. The circles and squares are the results for the 1.444- and 1.493-eV lines, respectively. The dotted curve indicates the laser profile. The profiles have been normalized by the intensity at 0 ns.

The radiative lifetime  $\tau_N$  of the exciton bound to the iso-electronic trap is expressed as<sup>42</sup>

$$\tau_N = 4.50 \frac{\lambda^2}{nf_N}, \quad (3)$$

$$f_N = \frac{\omega_{\text{ex}}}{\omega} \frac{4\pi\Lambda^3}{\Omega_{\text{mol}}} \left( \frac{m_h}{\mu_X} \right)^3 f_{\text{ex}}, \quad (4)$$

where  $\lambda$  is the wavelength of the transition in cm,  $f_N$  is the oscillator strength of the transition,  $n$  is the refractive index, and  $\omega_{\text{ex}}$  and  $\omega$  are the angular frequencies of the transition for the free and bound excitons, respectively.  $\Omega_{\text{mol}}$  is the volume of a GaAs molecule,  $m_h$  is the hole effective mass, and  $f_{\text{ex}}$  is the oscillator strength of a free exciton in GaAs. The calculated radiative lifetimes for the 1.444- and 1.493-eV lines are 12 and 1.1 ns, respectively. Here, the parameters for bulk GaAs are employed in Refs. 40, 41, 47, and 48. The ratio between the observed and calculated lifetimes,  $\tau_{\text{exp}}/\tau_{\text{calc}}$ , for the 1.493-eV line is larger than that for the 1.444-eV line. This result indicates that the assumption of the short-range potential for the electron is considered invalid for the 1.493-eV line because of the longer N-pair distance. This hypothesis is consistent with the expectation that the 1.444- and 1.493-eV lines can be attributed to the first- and fourth-nearest neighbor N pairs, respectively.

#### IV. CONCLUSIONS

In conclusion, we studied the magneto-PL and PL dynamics of excitons bound to N pairs in N  $\delta$ -doped GaAs. An extremely high uniformity for the emission wavelength of the exciton bound to the N pairs in the (001) plane was achieved; the homogeneous and inhomogeneous line widths were estimated to be approximately 70 and 15  $\mu\text{eV}$ , respectively. The uniformity of the emission wavelength suggests that the N  $\delta$ -doping technique is suitable for controlling the distribution of N-pair levels because of the controlled local-strain field of the  $C_{2v}$  symmetry. The magneto-PL spectra in the Faraday configuration showed the characteristic Zeeman interaction of the  $C_{2v}$  symmetry for the 1.493-eV line. On the other hand, the magneto-PL spectra suggested that the N pair for the 1.444-eV line was not aligned in the growth plane. The spatial distribution of the excitons localized at different N pairs was estimated by the diamagnetic shift coefficient and confirmed by the radiative lifetime of the bright-exciton component; the 1.444- and 1.493-eV lines can be attributed to the first- and fourth-nearest neighbor N pairs, respectively. The strong spatial localization of the bound exciton experimentally showed that both the short-range exchange interaction and the local strain field played key roles, in contrast to the well-known excitons confined in self-assembled QDs. The strong electron confinement for the 1.444-eV line results in the reduction of exciton-phonon interaction.

#### ACKNOWLEDGMENTS

This work was partially supported by the Grant-in-Aid for Scientific Research (Nos. 21360151 and 23656222) and

Young Scientists (No. 22760229) from the Ministry of Education, Culture, Sports, Science and Technology, Japan.

- <sup>1</sup>M. Weyers, M. Sato, and H. Ando, *Jpn. J. Appl. Phys.* **31**, L853 (1992).
- <sup>2</sup>W. Shan, W. Walukiewicz, J. W. Ager III, E. E. Haller, J. F. Geisz, D. J. Friedman, J. M. Olson, and S. R. Kurtz, *Phys. Rev. Lett.* **82**, 1221 (1999).
- <sup>3</sup>Y. Zhang and A. Mascarenhas, *Phys. Rev. B* **61**, 15562 (2000).
- <sup>4</sup>A. Patané, J. Endicott, J. Ibáñez, P. N. Brunkov, L. Eaves, S. B. Healy, A. Lindsay, E. P. O'Reilly, and M. Hopkinson, *Phys. Rev. B* **71**, 195307 (2005).
- <sup>5</sup>L. Xu, D. Patel, C. S. Menoni, J. Y. Yeh, L. J. Mawst, and N. Tansu, *Appl. Phys. Lett.* **89**, 171112 (2006).
- <sup>6</sup>G. Bentoumi, Z. Yaiche, R. Leonelli, J.-N. Beaudry, P. Desjardins, and R. A. Masut, *J. Appl. Phys.* **103**, 063526 (2008).
- <sup>7</sup>A. Polimeni, F. Masia, G. Pettinari, R. Trotta, M. Felici, M. Capizzi, A. Lindsay, E. P. O'Reilly, T. Niebling, W. Stolz, and P. J. Klar, *Phys. Rev. B* **77**, 155213 (2008).
- <sup>8</sup>L. Ivanova, H. Eisele, M. P. Vaughan, P. Ebert, A. Lenz, R. Timm, O. Schumann, L. Geelhaar, M. Dähne, S. Fahy, H. Riechert, and E. P. O'Reilly, *Phys. Rev. B* **82**, 161201(R) (2010).
- <sup>9</sup>M. Kondow, K. Uomi, A. Niwa, T. Kitatani, S. Watahiki, and Y. Yazawa, *Jpn. J. Appl. Phys.* **35**, 1273 (1996).
- <sup>10</sup>N. Tansu, N. J. Kirsch, and L. J. Mawst, *Appl. Phys. Lett.* **81**, 2523 (2002).
- <sup>11</sup>N. Tansu, J.-Y. Yeh, and L. J. Mawst, *Appl. Phys. Lett.* **83**, 2112 (2003).
- <sup>12</sup>S. R. Bank, M. A. Wistey, H. B. Yuen, L. L. Goddard, W. Ha, and J. S. Harris, *Electron. Lett.* **39**, 1445 (2003).
- <sup>13</sup>N. Tansu, J.-Y. Yeh, and L. J. Mawst, *J. Phys.: Condens. Matter* **16**, S3277 (2004).
- <sup>14</sup>R. Adams, *Electron. Lett.* **40**, 1086 (2004).
- <sup>15</sup>N. López, L. A. Reichertz, K. M. Yu, K. Campman, and W. Walukiewicz, *Phys. Rev. Lett.* **106**, 028701 (2011).
- <sup>16</sup>E. P. O'Reilly, A. Lindsay, P. J. Klar, A. Polimeni, and M. Capizzi, *Semi-cond. Sci. Technol.* **24**, 033001 (2009).
- <sup>17</sup>T. Kita and O. Wada, *Phys. Rev. B* **74**, 035213 (2006).
- <sup>18</sup>X. Liu, M.-E. Pistol, and L. Samuelson, *Phys. Rev. B* **42**, 7504 (1990).
- <sup>19</sup>T. Makimoto, H. Saito, T. Nishida, and N. Kobayashi, *Appl. Phys. Lett.* **70**, 2984 (1997).
- <sup>20</sup>R. Intartaglia, T. Taliercio, P. Valvin, B. Gil, T. Bretagnon, P. Lefebvre, M. A. Pinault, and E. Tournié, *Phys. Rev. B* **68**, 235202 (2003).
- <sup>21</sup>S. Francoeur, J. F. Klem, and A. Mascarenhas, *Phys. Rev. Lett.* **93**, 067403 (2004).
- <sup>22</sup>D. G. Thomas, J. J. Hopfield, and C. J. Frosch, *Phys. Rev. Lett.* **15**, 857 (1965).
- <sup>23</sup>D. G. Thomas and J. J. Hopfield, *Phys. Rev.* **150**, 680 (1966).
- <sup>24</sup>B. Gil, J. Camassel, P. Merle, and H. Mathieu, *Phys. Rev. B* **25**, 3987 (1982).
- <sup>25</sup>M. Ikezawa, Y. Sakuma, and Y. Masumoto, *Jpn. J. Appl. Phys.* **46**, L871 (2007).
- <sup>26</sup>T. Makimoto, H. Saito, and N. Kobayashi, *Jpn. J. Appl. Phys.* **36**, 1694 (1997).
- <sup>27</sup>P. R. C. Kent and A. Zunger, *Phys. Rev. B* **64**, 115208 (2001).
- <sup>28</sup>T. Kita, Y. Harada, and O. Wada, *Phys. Rev. B* **77**, 193102 (2008).
- <sup>29</sup>Y. Harada, O. Kojima, T. Kita, and O. Wada, *Phys. Status Solidi B* **248**, 464 (2011).
- <sup>30</sup>T. Ida, M. Ando, and H. Toraya, *J. Appl. Cryst.* **33**, 1311 (2000).
- <sup>31</sup>F. Ishikawa, M. Morifuji, K. Nagahara, M. Uchiyama, K. Higashi, and M. Kondow, *J. Cryst. Growth* **323**, 30 (2011).
- <sup>32</sup>Y. Harada, Y. Horiuchi, O. Kojima, T. Kita, and O. Wada, in *AIP Conference Proceedings, 30th International Conference on the Physics of Semiconductors*, edited by H. Cheong (American Institute of Physics, Melville, NY, in press).
- <sup>33</sup>S. N. Walck and T. L. Reinecke, *Phys. Rev. B* **57**, 9088 (1998).
- <sup>34</sup>S. Marcet, C. Ouellet-Plamondon, J. F. Klem, and S. Francoeur, *Phys. Rev. B* **80**, 245404 (2009).
- <sup>35</sup>D. Gammon, A. L. Efros, T. A. Kennedy, M. Rosen, D. S. Katzer, D. Park, S. W. Brown, V. L. Korenev, and I. A. Merkulov, *Phys. Rev. Lett.* **86**, 5176 (2001).
- <sup>36</sup>M. Erdmann, C. Ropers, M. Wenderoth, R. G. Ulbrich, S. Malzer, and G. H. Döhler, *Phys. Rev. B* **74**, 125412 (2006).
- <sup>37</sup>M. Abbarchi, T. Kuroda, T. Mano, K. Sakoda, and M. Gurioli, *Phys. Rev. B* **81**, 035334 (2010).
- <sup>38</sup>M.-F. Tsai, H. Lin, C.-H. Lin, S.-D. Lin, S.-Y. Wang, M.-C. Lo, S.-J. Cheng, M.-C. Lee, and W.-H. Chang, *Phys. Rev. Lett.* **101**, 267402 (2008).
- <sup>39</sup>M. Bayer, G. Ortner, O. Stern, A. Kuther, A. A. Gorbunov, A. Forchel, P. Hawrylak, S. Fafard, K. Hinzer, T. L. Reinecke, S. N. Walck, J. P. Reithmaier, F. Kloppe, and F. Schäfer, *Phys. Rev. B* **65**, 195315 (2002).
- <sup>40</sup>*Numerical Data and Functional Relationships in Science and Technology*, Landolt Börnstein, New Series, Group III, edited by O. Madelung and M. Schulz (Springer-Verlag, Berlin, 1987), Vol. 22a.
- <sup>41</sup>SOPRA N&K database, <http://www.sopra-sa.com>.
- <sup>42</sup>C. H. Henry and K. Nassau, *Phys. Rev. B* **1**, 1628 (1970).
- <sup>43</sup>L. Besombes, K. Kheng, L. Marsal, and H. Mariette, *Phys. Rev. B* **63**, 155307 (2001).
- <sup>44</sup>E. Peter, J. Hours, P. Senellart, A. Vasanelli, A. Cavanna, J. Bloch, and J. M. Gérard, *Phys. Rev. B* **69**, 041307(R) (2004).
- <sup>45</sup>S. Moehl, F. Tinjod, K. Kheng, and H. Mariette, *Phys. Rev. B* **69**, 245318 (2004).
- <sup>46</sup>R. Schwabe, W. Seifert, F. Bugge, R. Bindemann, V. F. Agekyan, and S. V. Pogarev, *Solid State Commun.* **55**, 167 (1985).
- <sup>47</sup>P. Chen, J. E. Nicholls, J. H. C. Hogg, T. Stirner, W. E. Hagston, B. Lunn, and D. E. Ashenford, *Phys. Rev. B* **52**, 4732 (1995).
- <sup>48</sup>I. Vurgaftman, J. R. Meyer, and L. R. Ram-Mohan, *J. Appl. Phys.* **89**, 5815 (2001).